

## Article

# Geochemical Characteristics of Typical Karst Soil Profiles in Anhui Province, Southeastern China

Wenbing Ji <sup>1,2</sup>, Yuanyuan Lu <sup>1,2</sup>, Min Yang <sup>1,2</sup>, Jian Wang <sup>1,2</sup>, Xiaoyu Zhang <sup>1,2</sup>, Caiyi Zhao <sup>1,2</sup>, Bing Xia <sup>1,2,3</sup>, Yunjin Wu <sup>1,2,\*</sup> and Rongrong Ying <sup>1,2</sup>

<sup>1</sup> Nanjing Institute of Environmental Sciences, Ministry of Ecology and Environment, Nanjing 210042, China; yrr@nies.org (R.Y.)

<sup>2</sup> State Environmental Protection Key Laboratory of Soil Environmental Management and Pollution Control, Nanjing 210042, China

<sup>3</sup> Research Academy of Environmental Sciences of Anhui Province, Hefei 230071, China

\* Correspondence: wyj@nies.org

**Abstract:** The geographical distributions of Cd and several other heavy metals (HMs) (Hg, Cu, Ni, Pb, Zn, Cr, As, Co, and V) were characterized in 90 ( $p > 0.05$ ) terra rossa samples across the Anhui karst area. Significant enrichment of HM was observed in this soil, mainly associated with the weathering of Cd-enriched carbonate rocks. Then, this enrichment was developed in 31 profiles. Our investigations revealed pedogenic processes as the dominant factors accounting for the enrichment of Hg, Cu, Ni, As, Co, and V. We also observed that all soil samples had a silty clay texture, with a pH scope of 4.08–8.04 and a median value of 6.50. In addition, the soil samples had relatively high saturation, with basic cations over 6.68%. The enrichment of the HMs based on their distinct factors were as follows: Cd (3.92) > As (2.55) > Zn (1.62) > Ni (1.50) > Cu (1.47) > Pb (1.47) > V (1.43) > Cr (1.23) > Co (1.19) > Hg (1.12). Finally, terra rossa samples derived from carbonate rocks were categorized as Cambisols, Luvisols, and Regosols. The soil profiles of Cambisols and Luvisols were less developed, so the HM concentrations were relatively low. The Regosols profile contained the highest total Cd concentration and exhibited a higher capacity to immobilize Cd compared with other soil profiles. Regosols are also characterized by high pH values (scope of 7.05 to 8.22, with an average value of 7.56). The contents of HM also exhibited minor changes across the Regosol, Cambisol, and Luvisol profiles, implying that the karst development degrees of weathering in Anhui were relatively low.

**Keywords:** karst areas; Anhui Province; heavy metals (HM); geochemical characteristics; enrichment factors



**Citation:** Ji, W.; Lu, Y.; Yang, M.; Wang, J.; Zhang, X.; Zhao, C.; Xia, B.; Wu, Y.; Ying, R. Geochemical Characteristics of Typical Karst Soil Profiles in Anhui Province, Southeastern China. *Agronomy* **2023**, *13*, 1067. <https://doi.org/10.3390/agronomy13041067>

Academic Editor: Jinman Wang

Received: 12 February 2023

Revised: 27 March 2023

Accepted: 3 April 2023

Published: 6 April 2023



**Copyright:** © 2023 by the authors. Licensee MDPI, Basel, Switzerland. This article is an open access article distributed under the terms and conditions of the Creative Commons Attribution (CC BY) license (<https://creativecommons.org/licenses/by/4.0/>).

## 1. Introduction

Carbonate rocks comprise sedimentary carbonate minerals (calcite, dolomite, etc.). The two major types of these rocks are limestone and dolomite. Soils formed mainly from carbonate rocks have a high geological background, owing to which such soil formations have received widespread attention in recent years [1–4]. In 2014, the National Soil Pollution Survey Bulletin showed that the soil environmental situation in China was deteriorating [5]. The report also indicated a gradual increase in the distribution of four harmful elements, such as Cd, Hg, Pb, As, Cu, Cr, Ni, and Zn, in the soil from different regions of China [5]. The Geochemical Survey Report of Chinese Farmland revealed that the proportion of points with moderate to severe heavy metal contamination or exceedance accounted for 2.5%, covering an area of 23,253 km<sup>2</sup> [6]. However, the proportion of points with slight to mild contamination or exceedance accounted for 5.7%, covering an area of 52,660 km<sup>2</sup>. In addition, the report also highlighted that the contaminated and exceeded arable land was mainly distributed in Hunan, Hubei, Anhui, Jiangxi, Fujian, Guangdong, and Hainan Provinces, as well as in Southwest China. Notably, Anhui Province in East China has vast

karst distributions, and is one of the many provinces where the heavy-metal content in soil is controlled by geological conditions. In China, that shows a regionalization trend, with the southwest region having a high concentration of different heavy metals (HM) [7]. Moreover, the average content of Cd and other HMs in the soils of karst areas in Guizhou and Guangxi Provinces was found to be much higher than the national average, causing the geologically high background of HM in these areas to be related to the content of the carbonate rocks in the soil [3,4,8].

Soils with a high geochemical background comprise soils that have accumulated abundant chemical elements due to geogenic processes and nearly no association with anthropogenic activities. Examples of geogenic processes include subsequent pedogenic processes. In terms of space, surface factors have a significant impact on the distribution of this soil. Comparative analysis shows that under specific conditions, soils with high geochemical background values generally show strong characteristics of heavy metal accumulation. Under other case, such soils are also featured by the high accumulation of bioavailable HM (e.g., in black rock areas) [9]. The geological background of elements indicates that the content of specific elements in the soil is independent of anthropogenic activities. Instead, these elements depend mainly on the initial elemental composition of the soil-forming parent rock and the geochemical processes of weathering, leaching, migration, and enrichment during soil formation [3,4,10].

Remarkably, carbonate rocks are widely distributed in Anhui, from the Aurignacian to the Early Triassic strata, with an outcropping area of about 8593 km<sup>2</sup> [11]. These rocks are also widely distributed in Huaibei, Suzhou, Chuzhou, Maanshan, Wuhu, Tongling, Chizhou, Huangshan, and Xuancheng Cities, as well as sporadically in other cities [11]. In Anhui Province, the soils derived from carbonate rock weathering materials are also distributed in the hilly mountainous areas of Jianghuai, covering an area of 3620 km<sup>2</sup>, which accounts for about 3.5% of the total soil area of the province [12]. However, the presence of HM in karst areas soils in Anhui Province continues to attract attention, particularly because Cd and other HMs in these soils dangerously exceed the standard levels [13]. A previous study investigated the ecological risk of elemental Cd in karst soils of the Qingyang County in Chizhou City, Anhui Province, and reported that the exceedance rate of Cd in rice seeds was as high as 41.67%, which was originally higher than that in non-karst areas [14].

In recent years, many scholars have also conducted systematic studies on the potential risks of HMs in the soils of karst areas, such as in Switzerland [15,16], Jamaica [17], southern Italy [1], Japan [18], and Southwest China [3,4]. In addition, studies have also examined the distribution characteristics of HMs and conducted risk evaluations of human health, soil enrichment mechanisms, and the biological effectiveness of soils in karst areas. HMs are apparently accumulated in karstic soils to varying degrees, in spite of the fact that the concentration distribution and migration characteristics of metals in soils derived from different parent rocks during the weathering process are different [4]. However, Anhui Province has received little research attention, because its typical karst distribution is relatively scattered and the degree of karst weathering development is low compared to other regions. As a result, no systematic investigation has been carried out for the whole Anhui Province, even though there are reports that have compared the HM content in soils from the karst areas of the province.

Moreover, there are limited studies on the distribution characteristics and enrichment mechanisms of HM in karst areas soils of Anhui Province, highlighting an urgent need to carry out relevant work in typical karst areas within the province. Therefore, in this report, the distribution pattern, enrichment mechanism, and migration characteristics of HM were investigated by comparing and analyzing soil profiles collected systematically from the carbonate distribution area of the Anhui Province.

## 2. Materials and Methods

### 2.1. Study Area

The Anhui Province is a transition zone between the north and the south of China, and serves as an important link between the eastern and the western parts of the country. Moreover, the province is long from north to south and narrow from east to west, with a large latitudinal span accounting for the climate changes from north to south in the sequence [19]. Investigations have also revealed that Anhui Province is a transitional area, between the warm temperate and subtropical zones, in terms of climate, whereas toward the south Huai River, the province has a subthermal humid monsoon climate [20]. Furthermore, the province has a distinct monsoon season, a warm spring, concentrated summer rains, a cool autumn, and a cold winter. The annual average temperature of the province is reported to be between 14.5 °C and 17.2 °C, with the lowest average temperature being in January and the highest in July [20]. However, while the annual temperature difference is greater in the north than in the south, the temperature rises and falls quickly in the spring and autumn, with few changes in temperature observed in the winter and summer.

According to the second Soil Census Statistics, the province mainly comprised 5 soil classes, 8 soil subclasses, 20 soil types, and 34 soil type subclasses [21]. However, the main soil classes observed in the province included yellow loam, brown loam, yellow-brown loam, red loam, yellow-red loam, sand ginger-black soil, paddy soil, coarse-bone soil, etc. The paddy soil accounted for the largest area of more than 10,000 km<sup>2</sup>, followed by sand ginger-black soil, red soil, tide soil, etc. Paddy soil, sand ginger-black soil, tide soil, and yellow-brown soil were also identified as the main cultivated soils, and were distributed in the Huabei plain, Jianghuai hilly area, and along the river plain. Soil distribution in Anhui Province has both horizontal and vertical zonalities, as well as regional distribution characteristics. Notably, the (yellow) tide and sand ginger-black soils were prevalent in the Huaibei Plain. The yellow-brown soil and paddy soil were dominant in Jianghuai Hills and Dabie Mountains. The paddy soil and gray-tide soil were dominant in the Yanjiang Plain, and the red soil and paddy soil developed from them were dominant in southern Anhui. Karst landforms mainly developed in the southern part of Anhui Province, dominated by mountains and hills, with relatively large terrain undulations.

### 2.2. Sampling and pre-Processing

The sampling methods adopted in this study were based on the agricultural land–soil sample collection flow preparation and preservation technology regulations [22]. Sampling sites included places where the soil type characteristics being mined were obvious, especially where the terrain was relatively flat, stable, and well-vegetated. The sampling sites are shown in Figure 1. We avoided locations with high interference from typical human activities, including areas where the land use type was mainly woodland. In this study, the sampling points were at least 300 m away from the railroad or highway; these points were based on the complete development of the profile and were placed at a clear level, without any invasive bodies. Places with serious erosion or topsoil destruction were avoided as sampling points. We also selected plots with no or little use of chemical fertilizers and pesticides as sampling points so that human activities would have less of an impact on the sample locations.

For this investigation, the coordinates of the actual sampling points were recorded by using a sampling handheld terminal and GPS (G630, Beijing UniStrong Technology Co. Beijing, China). The coordinates of each sampling point can be referenced in Table S2. The soil samples were collected from the A, B, and C layers in the general profile (Figure 2). The sampling order was from bottom to top. Next, samples were taken as far as possible with bamboo slices or knives to remove the soil in contact with the metal sampler, and then the profiles of the collected samples were assessed at about 1 kg per layer. As a result, 31 typical soil profiles were collected from the province, comprising 90 soil samples. These

soil types were identified as Cambisols, Luvisols, and Regosols, following the World Reference Base for Soil Resources [23] (Figure 2).

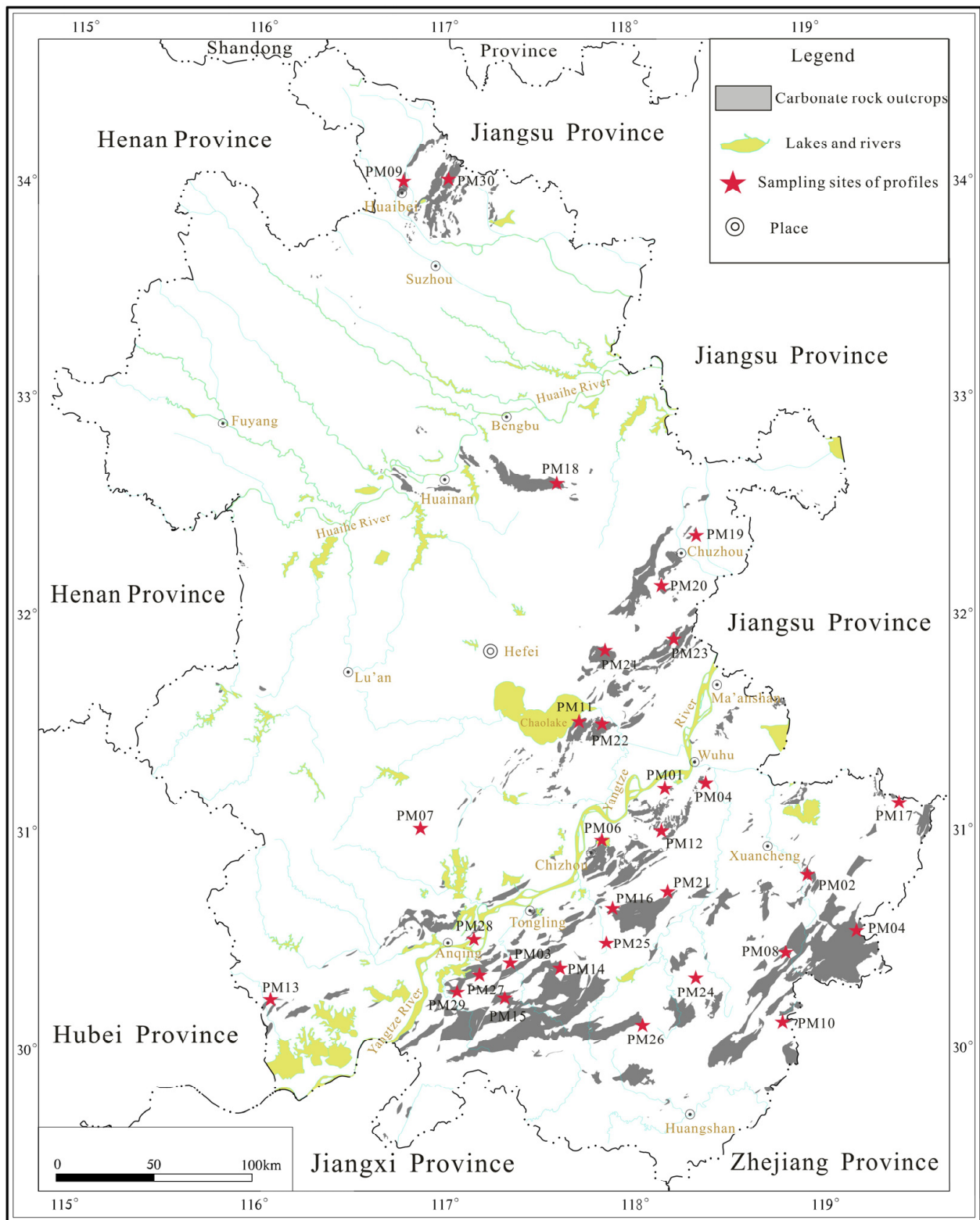
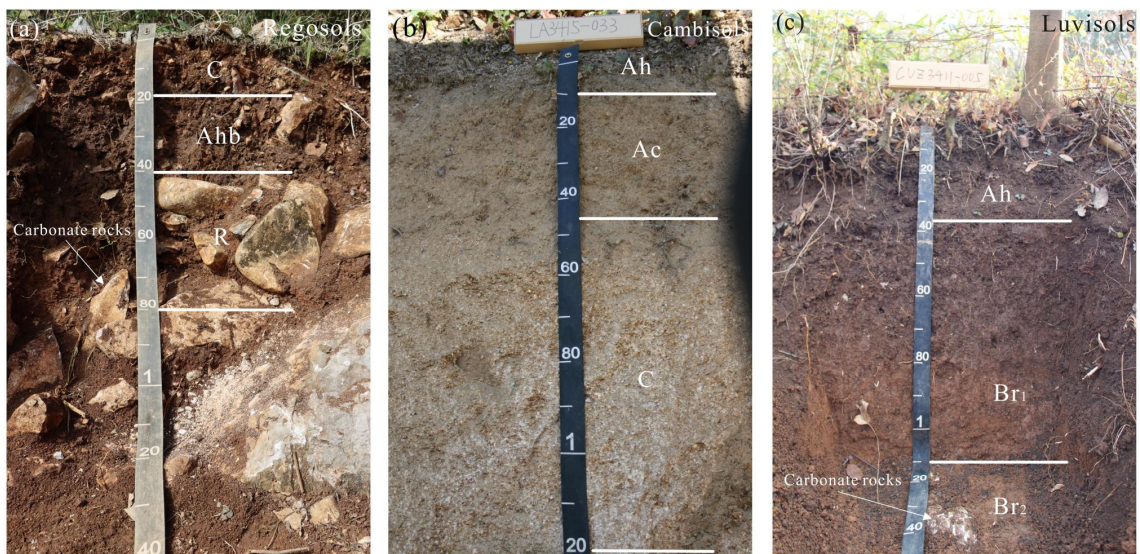


Figure 1. Schematic showing the sampling sites in the study area.





**Figure 2.** Diagram showing the typical profiles of Regosols (a), Cambisols (b), and Luvisols (c) in the study area.

The soil profiles of Regosols were generally shallow, with depths in the range of 20–45 cm, while both Cambisols and Luvisols were generally deep, with depths in the ranges of 25–120 cm and 40–120 cm (Figure S1). The main soil typology in all three of the types of soils was characterized by carbonate residual with calcium composition. The feature of such soil typology is the formation of a mollic horizon. The content of the insoluble material had a different mineral-to-organic ratio, probably causing the differing soil development in the study areas.

### 2.3. Chemical Analysis

In this study, the air-drying room was well-ventilated, clean, free of volatile chemicals, and built to avoid direct sunlight. During analysis, the air-dried sample was poured onto a Plexiglas plate in the sample-making room, then crushed with a wooden hammer and again with a wooden stick, followed by picking out impurities. Next, all the soil samples were hand-ground, mixed, and passed through a 2 mm nylon sieve to remove sand particles more than 2 mm in size. If the sand particle content was greater, the percentage of the whole soil sample with particles larger than 2 mm was calculated, and then the sample repeatedly ground and sieved until they all passed through. The sieved samples were fully mixed and stirred until uniform. Finally, while we obtained a small amount for testing (pH, organic matter, cation exchange amount, carbonate, and soil texture), other samples were continuously subjected to grinding with an agate ball mill until all were able to pass through a 0.15 mm (100 mesh) nylon sieve aperture, after which they were discarded in quadrature and bagged for analysis. The test method adopted in this study refers to the recommended analytical test method in the “Technical Provisions for the Analysis and Testing Method of Soil Samples for National Soil Pollution Status Detailed Investigation” [22]. The concentrations of Cd, Pb, Cr, Cu, Zn, Ni, Co, and V in the soil samples were determined using an inductively coupled plasma mass spectrometer (ICP-MS, Agilent, Palo Alto, USA), while Hg and As concentrations were determined by atomic fluorescence spectrophotometer (AFS, Beijing Jitian Instruments Company, Beijing, China), and Mn concentrations were determined by inductively coupled plasma emission spectrometer (ICP-OES, Agilent 5900, USA) after extraction with HCl–HNO<sub>3</sub>–HClO<sub>4</sub>–HF. The sample testing parameters and methods are shown in Table S1.

#### 2.4. Quality Control

The analytical quality control showed good precision in the study, because the specific analytical methods and detection limits adopted in this study for accuracy and precision were controlled using standard substances (GSB 04-2828-2011, GSB 04-1767-2004, and GSB 07-3159-2014) (China Geological Survey). The precision (relative deviation RSD/%) of the collected samples was less than 20%, and the accuracy (spiked recovery) was 90–110%.

#### 2.5. Data Processing and Statistical Analysis

Basic statistics were conducted to summarize major elements and trace metal concentrations in this area. To this end, while nonparametric tests were conducted based on SPSS 24 (IBM SPSS software, New York, NY, USA), the geographical distribution maps were generated based on ESRI-Arc GIS 10.5.

### 3. Results and Discussion

#### 3.1. Physical and Chemical Properties of Understudied Soils

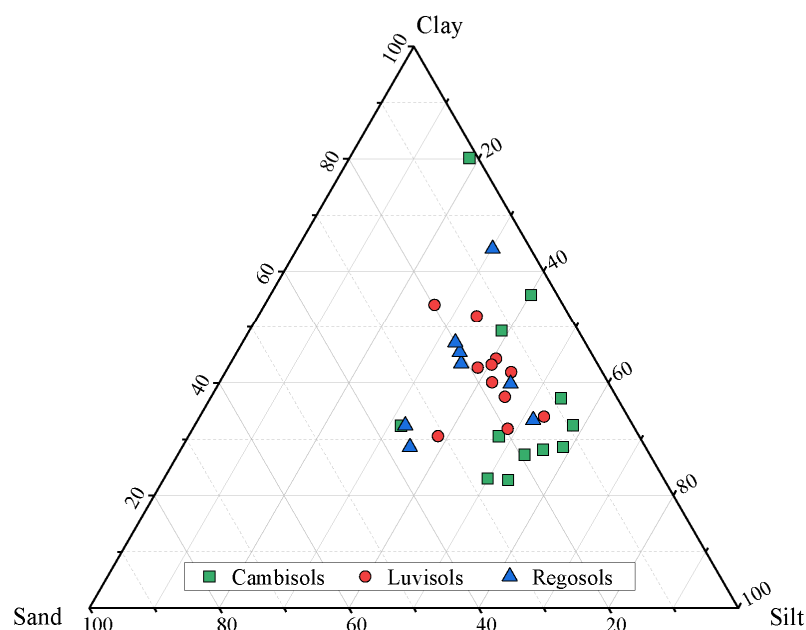
The soil pH in the study area was found to range from 4.08 to 8.44, with a median value of 6.50, suggesting that the study area had, overall, weakly acidic to weakly alkaline soil. We also detected 18 samples with pH values lower than 5.0, which accounted for 22.22%; 39 samples with pH values higher than 7.0, accounting for 43.33%; and 33 samples with pH values greater than 5.0 but less than 7.0, accounting for 36.67% (Table 1). Alternatively, studies have reported that climatic conditions significantly affect the pH and chemical composition of the soil [3,24]. To this end, we observed that the soil in the study area was relatively well hydrated and heated. However, water-soluble ions such as  $K^+$ ,  $Na^+$ ,  $Ca^{2+}$ , and  $Mg^{2+}$  were observed to be heavily leached during the development of parent material in the soil, resulting in some limestone soils being weakly acidic [25,26]. Conversely, the soil content was easily influenced by geological background, climate, agricultural activities, and land use, since soil organic matter mainly comes from plants, animals, and microbial residues [27]. Specifically, the karst areas have an extremely complex binary spatial heterogeneous structure, but their water–air–solid exchange conditions of carbon, vegetation conditions, and rock weathering features, as well as their topography, differ greatly from non-karst areas. A previous study reported that the spatial distribution of the soil's organic matter in karst areas exhibited unique characteristics [28]. The study also reported that the spatial variability of organic matter in soil in karst areas was greater than in other regions, and the influencing factors varied in different areas. In our study, the minimum value of soil organic matter in the study area was 0.27%, while the mean value was 2.86%. This finding is in agreement with the average soil organic matter content of 2.51% which was reported in Mashan County, Guangxi. In addition, we detected 42 samples with carbonate content in their soil profiles that had a detection rate of 46.67%, with their carbonate rock contents ranging from 0.6% to 84.9%, and their mean value was 4.79%. However, 48 samples were undetected, with a nondetection rate of 53.33%. This finding is in accordance with other studies which have reported the level of carbonate rock content in the soil to be closely related to the degree of soil profile development and sampling location [29,30]. Moreover, since the carbonate content in soil significantly correlates with pH, the soil samples with a relatively high carbonate content and pH were found to be predominant. This is in agreement with our study, where the texture of the soil in the study areas was mainly clay and chalky clay [3].

According to the American texture classification, the majority of the soil samples had silty clay (SC) textures (Figure 3). The sand content was the range of 16.3–64.8% (with an average of 42.52%); silt was in the range of 0.1–41.4% (with an average of 16.79%); and clay was in the range of 20.1–81.4% (with an average of 40.5%).

**Table 1.** Physical and chemical properties of the soil profile in the study area.

Items	Number of Samples	Min	Max	Average	Med	Std	CV <sup>(a)</sup>
pH	/	4.08	8.44	6.50	6.83	1.30	0.20
SOM	%	0.27	9.17	2.86	2.32	2.05	0.72
CEC	Cmol (+)/kg	6.68	47.7	26.55	23.7	9.53	0.36
BD	g/cm <sup>3</sup>	0.62	1.71	1.25	1.27	0.60	0.48
Carbonate	%	90 <sup>(c)</sup>	Nd	84.9	2.44	Nd	9.50

<sup>(a)</sup> Coefficient of variation = standard deviation/mean; <sup>(b)</sup> only some soil profiles were tested for capacitance; <sup>(c)</sup> 90 samples were tested for carbonate content, of which 42 were detected, and 48 were below the detection limit of 46.67%. SOM: soil organic matter. CEC: cation exchange capacity. BD: bulk density. CV: coefficient of variation.

**Figure 3.** Particle size distributions of soils with different profiles.

### 3.2. Geochemical Anomalies of Cd and other HM

The statistical results regarding the Cd, Cu, As, Hg, Cr, and V concentrations in the terra rossa from the weathering profiles in the study area can be seen from Table 2. According to the results of other research, Cd and other HMs were obviously enriched in soils which originated from carbonate rocks in the Anhui Province's karst areas [13,31,32]. Therefore, this paper compared their content with the national background values of soils (BVS) to assess the metal levels in terra rossa [33]. Our findings revealed that in the samples, the HM levels exceeded the BVS in this order: V (94.44%) > As (93.33%) > Cd (87.78%) > Ni (86.67%) > Zn (85.56%) > Cr (77.78%) > Co (77.78%) > Cu (72.22%) > Pb (53.33%) > Hg (47.78%). However, in the typical southwest karst region of China, the sequence is as follows: Cd (100%) > Cr (95.2%) > Pb (88.0%) > Zn (83.8%) > Ni (65.6%) [4]. These results highlight the reasons why the evaluation of the mechanism of abnormal cadmium enrichment and potential ecological risks in karst areas has received wide attention [3,4,9].

The Cd content in terra rossa in that area was the highest, with the mean Cd content being 2.84 times higher than in the overall province. In addition, the average concentration of Cd was 2.84 times greater than the nation BVS (Table 2). Moreover, the Cd contents in terra rossa were higher, with the average Cd concentrations being 2.99 and 1.09 times higher compared to the national average values (Table 2). Similar characteristics of the soil were also observed in the karst region of Southwest China [4]. Notably, the main rock-forming minerals in the carbonate rocks were calcite and dolomite, which rapidly leach and decompose during weathering and soil formation. This leaching and decomposition results in a huge loss of volume and mass, thus showing low background and high

enrichment [4,34]. The  $\text{Cd}^{2+}$  ( $0.97 \text{ \AA}$ ) level was similar to that of  $\text{Ca}^{2+}$  ( $0.99 \text{ \AA}$ ), indicating that Cd can replace Ca in carbonate minerals analogously. Therefore, in most carbonates, Cd is predominantly hosted in the carbonate mineral phase [30].

In contrast, the enrichment factors of other HMs were as follows: As (2.55) > Zn (1.62) > Ni (1.50) > Cu (1.47) > Pb (1.47) > V (1.43) > Cr (1.23) > Co (1.19) > Hg (1.12). The main reason for this trend was that these profiles were located in eastern areas. These areas were found to have slightly higher Cd anomalies [35]. Our investigations also revealed that the concentrations of Pb, Cu, Ni, and Cr in terra rossa were slightly higher compared to the national BVS. The Cd content can be rather high in some specific areas, although the Cd content in carbonate rocks is generally low, with the average value being  $0.035 \text{ mg}\cdot\text{kg}^{-1}$  worldwide [35]. For instance, Cd anomalies in Switzerland have been reported to  $0.28 \text{ mg}\cdot\text{kg}^{-1}$ , with other HMs such as Zn, Pb, and Cr also being unusually enriched [3,4,36]. Cd anomalies also appeared in the Three Gorges in Southwestern China [37].

Our statistical research found that the Cd anomaly in local carbonate rocks in Anhui Province had a mean of  $0.12 \text{ mg}\cdot\text{kg}^{-1}$ , which is 3.43 times higher than the average Cd concentration in carbonate rocks across the world. Notably, the mean contents of Cu, Pb, Zn, and Cr in the sample were higher compared to their worldwide carbonate rock contents. However, the mean content of Ni in local carbonate rocks was lower compared to the reference (Table 2). According to the result in Table 2, the contents of Cd, Cu, and As in deep soils were higher than in topsoil in the local karst areas. This could be because the differential weathering of the residual detrital minerals had no obvious impact on the mobilization of trace metals in saprolites during the weathering of Cd-enriched parent rocks [4]. Therefore, while the dominant factor of Cd enrichment in terra rossa was the anomalously high Cd content in carbonate bedrock, the contents of Cu, Ni, Pb, Zn, and Cr were highly enriched during pedogenesis.

**Table 2.** HM concentrations (mg/kg) in terra rossa from the weathering profiles across the study area.

Sample	Cd	Cu	Ni	Pb	Zn	Cr	Hg	As	Co	V	References
Terra rossa ( $n = 90$ , from profiles)	$0.38 \pm 0.35$ (0.04–1.53)	$33.35 \pm 20.72$ (0.03–112)	$40.48 \pm 15.07$ (13–103)	$38.27 \pm 33.34$ (8.8–179)	$120.18 \pm 50.11$ (63.1–263)	$75.08 \pm 28.88$ (27–246)	$0.073 \pm 0.05$ (0.02–0.22)	$28.6 \pm 18.21$ (8.07–96.8)	$15.1 \pm 3.53$ (5.49–22.9)	$117.58 \pm 31.41$ (74.2–211)	This study
Carbonate rock in Shitai County in Anhui	0.12	19.84	2.84	14.9	38.41	382.22	0.08	10.64			[31]
Topsoils in Shitai County	0.30	42.69	42.94	29.62	112.58	103.91	0.13	19.33			[31]
Deep soils in Shitai County	0.50	46.24	35.81	31.2	93.54	82.3	0.09	21.17		203.71	[31]
Background soil (Anhui)	0.134	26	28	27	64	70	0.048	9.5	14.3	85	[31]
World carbonate rock	0.035	4.0	20.0	9.0	20.0	11.0	0.16	1	0.1	45	[38]
Background soil (China)	0.097	22.6	26.9	26.0	74.2	61.0	0.07	11.2	12.7	82.4	[33]
Background soil (Guangxi)	0.27	27.8	26.6	24.0	75.6	82.1					[4]
World soil	0.35	30.0	20.0	19.0	90.0	40.0					[39]
Chinese soil	0.23	27.1	29.6	31.2	79.0	68.5					[40]



Table 2. Cont.

Sample	Cd	Cu	Ni	Pb	Zn	Cr	Hg	As	Co	V	References
Chinese soil (first environmental soil background values)	0.127	24	29	27	67	68	0.05	10.8	13	87	[41]
Carbonate rock in Guangxi	0.374	1.89	5.15	3.86	10.7	11.9	0.01	0.94			[9]
Enrichment factors *	3.92	1.47	1.50	1.47	1.62	1.23	1.12	2.55	1.19	1.43	

\* Enrichment factors = calculated as the ratio of the concentration of the element in the soil to the national background values (BVS) [33].

### 3.3. Geographical and Soil Type-Dependent Distributions of HM in Terra Rossa

Carbonate rocks can be categorized into many soil types based on the process of weathering into loam, the degree of weathering, conditions of the parent material, climatic conditions, and other factors [3,4]. In addition, the distributions of HMs such as Cd, Hg, Cu, Zn, Cr, As, Co, and V in Cambisols, Luvisols, and Regosols have been reported to be higher than the national BVS [33] (Figure 4).

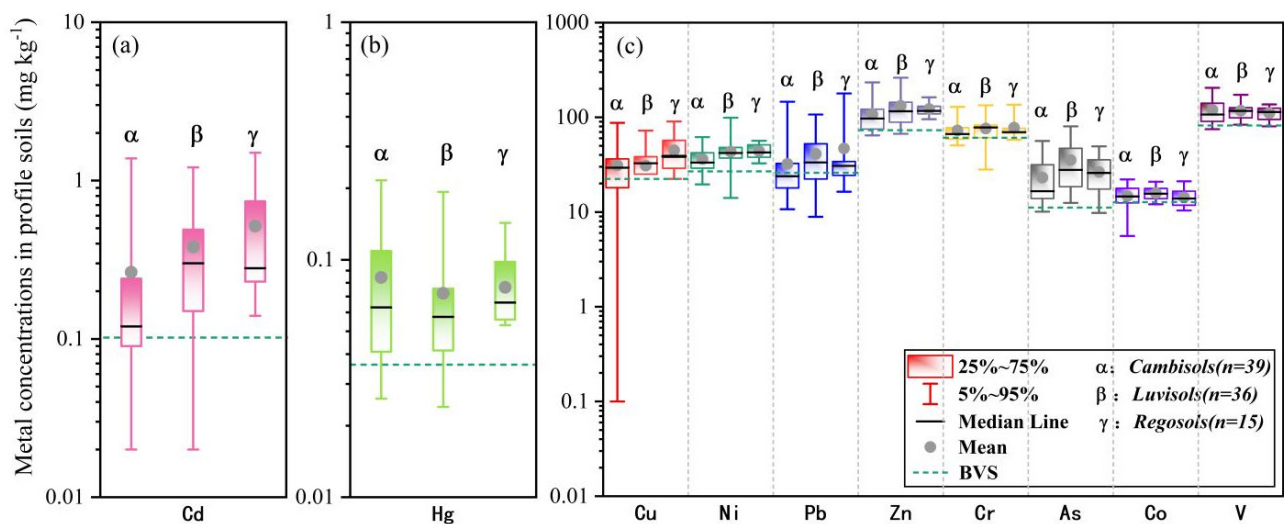


**Figure 4.** Soil type-dependent distributions of (a) Cd; (b) Hg; and (c) Cu, Ni, Pb, Zn, Cr, As, Co, and V in terra rossa ( $n = 90$ ). Bold lines denote the national BVS [33].

A previous study described the two climatic zones of Anhui Province, of which the south of the Huai River has a subthermal humid monsoon climate [19]. Accordingly, distributions of total Cd (Figure 4a) and other metals (Figure 4b,c) in terra rossa were dependent on the soil type. Regosols contained the highest total Cd concentration and had high pH values (7.05 to 8.22, average value 7.56), accounting for their higher capacity to immobilize Cd [42]. Regosols also represent a very weakly developed soil type, in which the coarse material showed almost no weathering in thin sections [42].

In contrast, Cambisols contained the lowest total Cd content and exhibited the feature of low pH values (4.57 to 7.17, mean 5.83). Therefore, they demonstrated a lower capacity to immobilize Cd [43]. HMs, such as Cu, Ni, Cr, in Cambisols exhibited similar characteristics to those of Cd, while Zn, Co, and V showed no significant differences ( $p > 0.05$ ). Generally, the distributions of total As in Luvisols are higher than in Cambisols and Regosols. In addition, studies have revealed that the bedrock surface of the weathering crust is strongly undulating due to the high solubility of carbonate rocks and their significantly differential

dissolution. As a result, a relatively narrow and abruptly changed alkaline barrier is formed in the rock–soil interface, while the boundary of the rock–soil interface is clear and abruptly changed [44–47].

### 3.4. Soil Type-Dependent Distributions of HM in the Soil Profile

Our results showed heavy metal concentrations in the soil vertical profile of the karst area in Anhui Province that varied significantly according to soil type (Figure S1). The thicknesses of 8 soil profiles were less than 57.5 cm in Regosols, and most of these profiles were collected from topsoil (0–20 cm). The number of collected samples ranged from 1 to 3 per soil profile. HMs also showed a small degree of variation in the soil profiles. Notably, Cd showed an increasing trend with the increase in the depth of the study area (Figures 5–7). The highest Cd content was found in the surface layer of PM26, with a maximum value of 1.50 mg/mg, which was much higher than the background values of Chinese soils and the background values of Anhui soils (0.134 mg/kg). In contrast, a decreasing trend of As content was observed with the increasing depth of the study area. The two variables had an obvious negative correlation, from which it was judged that stratigraphic factors would have a significant impact on the enrichment of this metal. However, the specific mechanism of its impact is still not very clear, and needs to be studied further. The highest As content was found in the surface layer of PM26, with the maximum value being 49.4 mg/kg, which was much higher compared to the background values of Chinese soils (11.2 mg/kg) and those of Anhui soils (9.5 mg/kg). In addition, the contents of As and Cd showed different characteristics that were closely related to their geochemical characteristics and major elements, such as Fe and Mn [44–47]. A study reported that Fe oxides, such as ferrihydrite and goethite, occur in many soils [47]. Ferrihydrite can be seen as an “amorphous Fe hydroxide,” and has the feature of short-range-ordered structure [48]. Moreover, biotic oxidations contribute to Mn/Fe oxide formation. The transport capacity of Cd in soils, like other HMs, depends mainly on its physicochemical processes in different phases of the soil environment [48–51]. For example, while Mn in Fe–Mn nodules significantly influenced the geochemical behavior of Cd, Co, Cu, and Ni, the presence of Fe significantly influenced the geochemical behavior of As, Cr, and V [25,48,52]. The contents of other HMs showed no significant variations with depth.

The thicknesses of 12 soil profiles were less than 110 cm in Cambisols, and the HMs (Cd, Cr, As, and V) showed regular variation with depth. Remarkably, Cd showed an increasing trend with the increase in the depth of the study area (Figure 6). The highest Cd content was observed in the surface layer of PM12, with the maximum value being 1.53 mg/mg, which was much higher compared to the background values of Chinese soils (0.097 mg/kg) and those of Anhui soils (0.134 mg/kg). In addition, a PM1 depth of 82.5 cm showed a clear inflection point where the contents of HM (Cu, Ni, Zn, Cr, Hg, and V) increased significantly, resulting in the formation of a typical geochemical barrier. Conversely, a decreasing trend of As content was observed with the increasing depth of the study area. The highest As content was observed in the surface layer of PM07, with the maximum value being 71.5 mg/mg, which was much higher than the background values of Chinese soils (11.2 mg/kg) and those of Anhui soils (9.5 mg/kg). However, the contents of other HMs (Ni, Pb, Zn, Cr, Co, and V) showed no significant variations with depth.

The thicknesses of 11 soil profiles in Luvisols were less than 105 cm, and the HMs (Pb, Zn, Cr, Co, V, and As) showed no significant variation with the changes in depth (Figure 7). Notably, the highest Cd content was found in the surface layer of PM16, with the maximum value being 1.23 mg/mg. This maximum value of Cd content was much higher compared to the background values of Chinese soils (0.097 mg/kg), those of Anhui soils (0.134 mg/kg), and those of carbonate rocks (0.12 mg/kg) in Shitai County, Anhui.

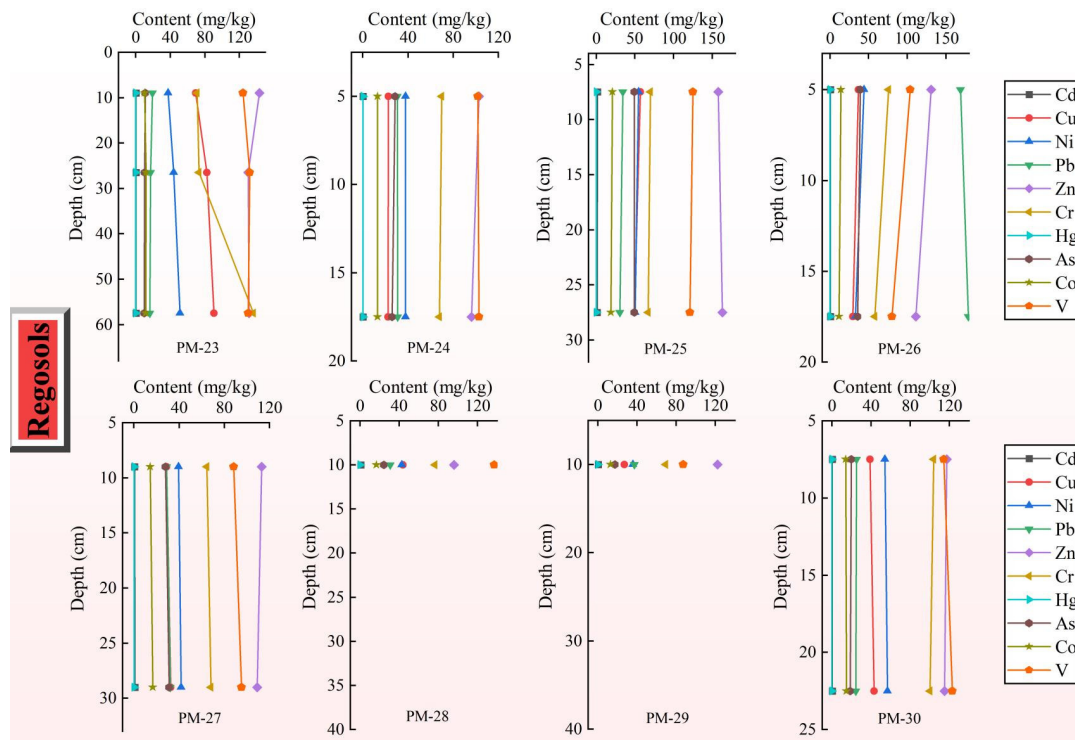


**Figure 5.** Distributions of HMs (Cd, Hg, Cu, Ni, Pb, Zn, Cr, As, Co, and V) in the Regosols profile ( $N = 8$ ).

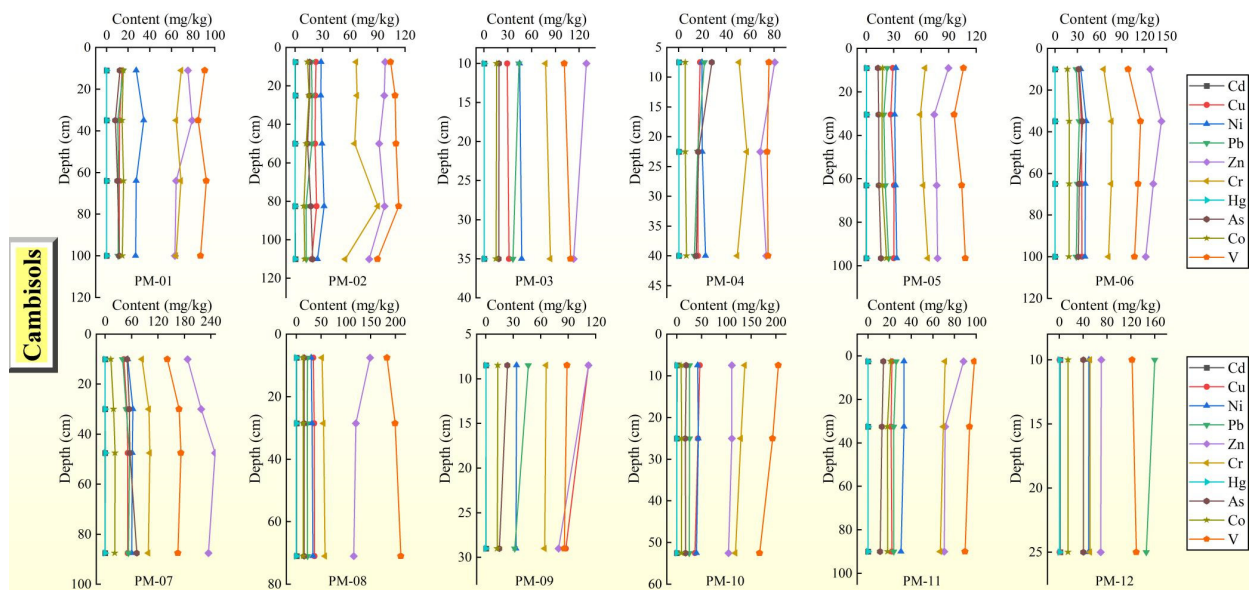


**Figure 6.** Distributions of HMs (Cd, Hg, Cu, Ni, Pb, Zn, Cr, As, Co, and V) in the Cambisols profile ( $N = 12$ ).

The geochemical properties of HM determine, to a certain extent, their migration ability as part of the weathering profiles. This is likely the reason why the weathering profiles in the study area showed a strong migration of Ni and a weak migration of Pb and As. We also observed that the geochemistry of As differed from that of other HMs. The element As was found to be present in soils as As(III) and As(V) in epigenetic environments, and was more prone to forming arsenates and arsenites. Moreover, the relatively low mobility of As in the various profiles of the study area indicates that Fe and Al oxides in the acidic Fe-rich and Al-rich soils of southern China readily associated with  $AsO_4^{3-}$  and combined with

AsO. This observation also indicates the relatively low mobility of As in the study area, reflecting that Fe and Al oxides in the acidic Fe-rich and Al-rich soils of southern China readily combine with  $\text{AsO}_4^{3-}$  to form insoluble salts such as Fe and Al arsenates [46,48].

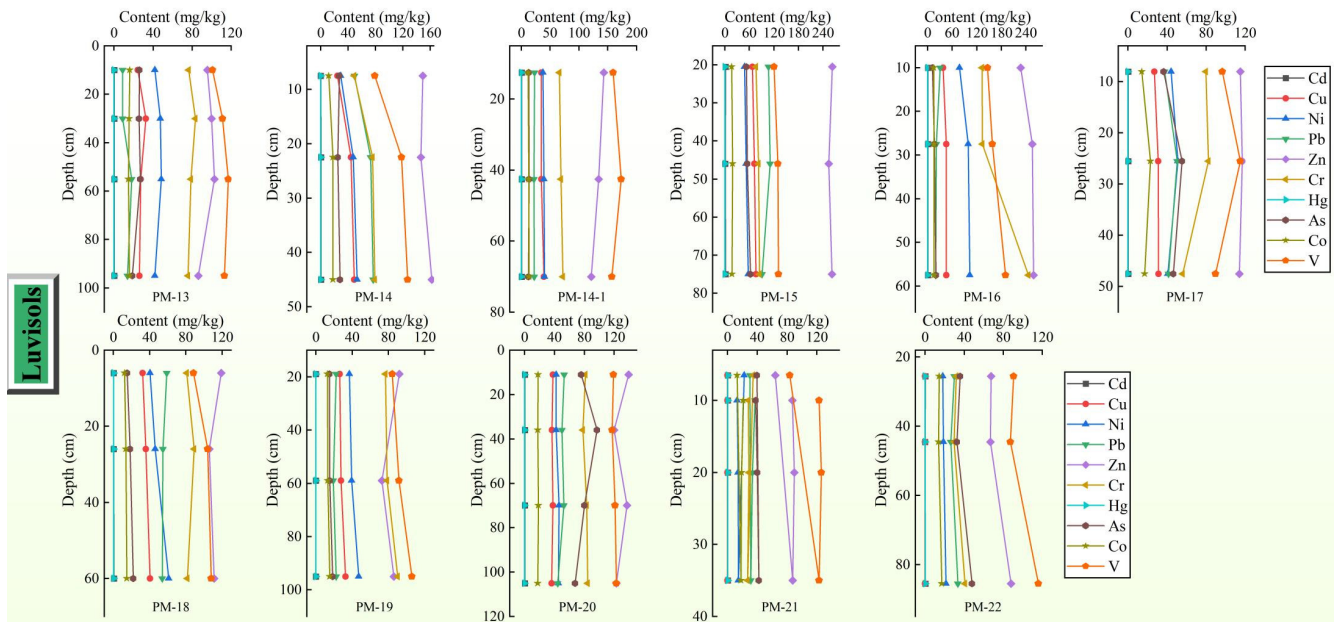


**Figure 7.** Distributions of HM (Cd, Hg, Cu, Ni, Pb, Zn, Cr, As, Co, and V) in the Luvisols profile ( $N = 11$ ).

Generally, the HM contents (Cd, Hg, Zn, Cr, and V) showed small changes across the Regosol, Cambisol, and Luvisol profiles, indicating the low karst development degrees of weathering in Anhui. This finding was further supported by the fact that no Fe-Mn nodules were observed in the 31 profiles obtained from this karst area.

#### 4. Conclusions

This paper researched the geographical distribution features of HMs based on the diversity of soil types in the karst areas of Anhui Province. First, our investigation revealed the elevated concentrations of Cd and other HMs in soils from the Anhui karst region. These elevated findings were likely due to weathering of the underlying carbonate rocks, including the subsequent pedogenic processes that occurred in this region. The terra rossa derived from carbonate rocks was categorized into Cambisols, Luvisols, and Regosols. Notably, Regosols exhibited high pH values and contained the highest total Cd concentration, suggesting that they have a greater capability to immobilize Cd compared to other soil types. Moreover, the HM content showed small changes across Regosols, Cambisols, and Luvisols profiles, implying that the karst weathering degree in Anhui was not high. Overall, our findings indicate that the combination of parent rocks, climatic conditions, and soil-forming effects on the weathering process of carbonate rocks ultimately leads to the relatively low background and high enrichment characteristics of HMs.

**Supplementary Materials:** The following supporting information can be downloaded at: <https://www.mdpi.com/article/10.3390/agronomy13041067/s1>, Figure S1: Soil profile development on different soils; Table S1: Sample testing parameters and methods; Table S2: The basic information of sampling point.



**Author Contributions:** Data curation, J.W.; formal analysis, M.Y.; funding acquisition, Y.W.; investigation, X.Z., C.Z. and R.Y.; methodology, W.J. and Y.L.; project administration, Y.W.; resources, W.J. and R.Y.; validation, W.J.; writing—original draft, W.J. and R.Y.; writing—review and editing, B.X. All authors have read and agreed to the published version of the manuscript.

**Funding:** This study was financially supported by the Integration of pollution prevention technology system for chemical park site zoning classification (2019YFC1804005).

**Data Availability Statement:** No data was used for the research described in the article.

**Conflicts of Interest:** The authors declare no conflict of interest.

## References

1. Vingiani, S.; Iorio, E.D.; Colombo, C.; Terribile, F. Integrated study of Red Mediterranean soils from Southern Italy. *Catena* **2018**, *168*, 129–140. [CrossRef]
2. Zupancic, N.; Turniski, R.; Miler, M.; Grcman, H. Geochemical fingerprint of insoluble material in soil on different limestone formations. *Catena* **2018**, *170*, 10–24. [CrossRef]
3. Wen, Y.B.; Yang, Z.F.; Zhuo, X.X.; Guan, D.X.; Song, Y.X.; Guo, C.; Ji, J.F. Evaluation of various approaches to predict cadmium bioavailability to rice grown in soils with high geochemical background in the karst region, Southwestern China. *Environ. Pollut.* **2020**, *258*, 113645. [CrossRef] [PubMed]
4. Wen, Y.B.; Li, W.; Yang, Z.F.; Zhang, Q.Z.; Ji, J.F. Enrichment and source identification of Cd and other heavy metals in soils with high geochemical background in the karst region, Southwestern China. *Chemosphere* **2020**, *245*, 125620. [CrossRef]
5. Ministry of Nature Resources of the Republic of China (MNR); Ministry of Environmental Protection (MEP). A National Soil Pollution Survey Bulletin. 2014. Available online: [http://www.gov.cn/xinwen/2014-04/17/content\\_2661765.htm](http://www.gov.cn/xinwen/2014-04/17/content_2661765.htm) (accessed on 11 February 2023).
6. Ministry of Nature Resources of the Republic of China. *Report on Geochemical Survey of Cultivated Land in China*; Ministry of Nature Resources of the Republic of China: Beijing, China, 2015. Available online: <https://www.cgs.gov.cn/xwl/ddyw/201603/t20160309302254.html> (accessed on 11 February 2023).
7. Luo, Y.M.; Teng, Y. Regional Difference in Soil Pollution and Strategy of Soil Zonal Governance and Remediation in China. *Bull. Chin. Acad. Sci.* **2018**, *33*, 145–152.
8. Ji, W.B.; Yang, Z.F.; Yu, T.; Yang, Q.; Wen, Y.B.; Wu, T.S. Potential ecological risk assessment of heavy metals in the Fe–Mn nodules in the karst area of Guangxi, Southwestern China. *Bull. Environ. Contam. Toxicol.* **2021**, *106*, 51–56. [CrossRef] [PubMed]
9. Yang, Q.; Yang, Z.F.; Zhang, Q.Z.; Liu, X.; Zhuo, X.X.; Wu, T.S.; Wang, L.; Wei, X.J.; Ji, J.F. Ecological risk assessment of Cd and other heavy metals in soil-rice system in the karst areas with high geochemical background of Guangxi, China. *Sci. China Earth Sci.* **2021**, *51*, 1317–1331. [CrossRef]
10. Baize, D.; Sterckeman, T. Of the necessity of knowledge of the natural pedo-geochemical background content in the evaluation of the contamination of soils by trace elements. *Sci. Total Environ.* **2001**, *264*, 127–139. [CrossRef] [PubMed]
11. Yao, Z.B.; Bi, Z.G.; Li, Z.K.; Chen, X.Y.; Xia, G.S. *Regional Geology of Anhui Province*; Geological Press: Beijing, China, 1987; pp. 209–214.
12. Gu, Y.P. Classification reference of carbonate developed soils in Anhui Province. *Soil Bull.* **1999**, *4*, 53–56.
13. Zhou, J.; Zhu, J.; Cha, S.X.; Han, Z.Y.; Qin, Y. Relationship between soil trace element status and geological background in Anhui Province. *J. Anhui Agric. Univ.* **2001**, *24*, 59–64.
14. Zhang, W. Soil Heavy Metal Enrichment Characteristics and Ecological Risk Assessment in Carbonate Background Area of Qingyang, Anhui Province. Master's Thesis, China University of Geosciences, Beijing, China, 2020.
15. Atteia, O.; Thélin, P.; Pfeifer, H.R.; Dubois, J.P.; Hunziker, J.C. A search for the origin of cadmium in the soil of the Swiss Jura. *Geoderma* **1995**, *68*, 149–172. [CrossRef]
16. Dubois, J.P.; Okopnik, F.; Benitez, N.; Védry, J.C. Origin and spatial variability of cadmium in some soils of the Swiss Jura. In Proceedings of the 16th World Congress Soil Science, Montpellier, France, 20–26 August 1998.
17. Lalor, G.C. Review of cadmium transfers from soil to humans and its health effects in the Jamaican environment. *Sci. Total Environ.* **2008**, *400*, 162–172. [CrossRef] [PubMed]
18. Yamasaki, S.-I.; Takeda, A.; Nunohara, K.; Tsuchiya, N. Red soils derived from limestone contain higher amounts of trace elements than those derived from various other parent materials. *Soil Sci. Plant Nutr.* **2013**, *59*, 692–699. [CrossRef]
19. Zhang, T.; Xu, W.X.; Lin, X.N.; Yan, H.L.; Ma, M.; He, Z.Y. Assessment of heavy metals pollution of soybean grains in North Anhui of China. *Sci. Total Environ.* **2019**, *646*, 914–922. [CrossRef] [PubMed]
20. China NBoSo. *China Statistical Yearbook*; China Statistics Press: Beijing, China, 2011.
21. Li, H.; Luo, N.; Li, Y.W.; Cai, Q.Y.; Li, H.Y.; Mo, C.H.; Wong, M.H. Cadmium in rice: Transport mechanisms, influencing factors, and minimizing measures. *Environ. Pollut.* **2017**, *224*, 622–630. [CrossRef]
22. Ministry of Ecology and Environment of the People's Republic of China. *Technical Provisions for the Analysis and Testing Method of Soil Samples for National Soil Pollution Status Detailed Investigation*; Ministry of Ecology and Environment of the People's Republic of China: Beijing, China, 2017.

23. Food and Agriculture Organization of the United Nations (FAO). *World Reference Base for Soil Resources 2014. International Soil Classification System for Naming Soils and Creating Legends for Soil Maps*; FAO: Rome, Italy, 2015.
24. Gong, Z.T. *Classification of Chinese Soil Systems*; Science Press: Beijing, China, 1999; pp. 903–907.
25. Ji, W.B.; Yang, Z.F.; Yin, A.J.; Lu, Y.Y.; Ying, R.R.; Yang, Q.; Liu, X.; Li, B.; Duan, Y.R.; Wang, J. Geochemical characteristics of Fe-Mn nodules with different sizes in soils of high geological background areas. *Chin. J. Ecol.* **2021**, *40*, 2289–2301.
26. Ji, W.B.; Yang, Z.F.; Yin, A.J.; Lu, Y.Y.; Ying, R.R.; Yang, Q.; Liu, X.; Li, B.; Duan, Y.R.; Wang, J. Study on the formation mechanism of iron-manganese nodules in soils with high geological background-taking the central part of Guangxi as an example. *Chin. J. Ecol.* **2021**, *40*, 2302–2314.
27. Zhong, C.; Li, X.J.; He, Y.Y.; Qiu, W.W.; Li, J.; Zhang, X.Y.; Hu, B.Q. Spatial variability of soil organic matter in Guangxi and its influencing factors. *Geoscience* **2020**, *40*, 478–484.
28. Zhang, C.L.; Lu, L.M.; Yang, H.; Huang, F. Spatial variation analysis of soil organic matter in karst area. *Carsologica Sin.* **2022**, *41*, 228–232.
29. Tang, S.Q.; Liu, X.J.; Yang, K.; Guo, F.; Yang, Z.; Ma, H.H.; Liu, F.; Peng, M.; Li, K. Migration, Transformation Characteristics, and Ecological Risk Evaluation of Heavy Metal Fractions in Cultivated Soil Profiles in a Typical Carbonate-Covered Area. *Environ. Sci.* **2021**, *42*, 3913–3923.
30. Wang, Q.Y. Study on the Characteristics of Heavy Metal Migration and Enrichment and Environmental Risk Assessment during the Weathering of Carbonate Rocks. Master's Thesis, Guizhou University, Guizhou, China, 2021.
31. Lu, C.M. Geochemical characteristics of rocks and soils in the Dashan area of Shitai, Anhui Province. *Anhui Geol.* **2010**, *20*, 120–125.
32. Zhou, J.; Hu, L.J.; Zhu, J.; Qin, Y. Geological background of agriculture in Qingyang and surrounding areas in southern Anhui. *Anhui Geol.* **1999**, *9*, 156–160.
33. China National Environmental Monitoring Centre (CNEMC). *Elemental Background Values of Soils in China*; Environmental Science Press: Beijing, China, 1990.
34. Yang, Q.; Yang, Z.F.; Filippelli, G.M.; Ji, J.F.; Ji, W.B.; Liu, X.; Wang, L.; Yu, T.; Wu, T.S.; Zhuo, X.X.; et al. Distribution and secondary enrichment of heavy metal elements in karstic soils with high geochemical background in Guangxi, China. *Chem. Geol.* **2021**, *567*, 120081. [[CrossRef](#)]
35. Xie, X.J. *Geochemical Atlas of China*; GPH: Springfield, MO, USA, 2012.
36. Quezada-Hinojosa, R.P.; Föllmi, K.B.; Verrecchia, E. Speciation and multivariable analyses of geogenic cadmium in soils at Le Gurnigel, Swiss Jura Mountains. *Catena* **2015**, *125*, 10–32. [[CrossRef](#)]
37. Liu, Y.; Xiao, T.; Perkins, R.B.; Zhu, J.; Zhu, Z.; Xiong, Y.; Ning, Z. Geogenic cadmium pollution and potential health risks, with emphasis on black shale. *J. Geochem. Explor.* **2017**, *176*, 42–49. [[CrossRef](#)]
38. Salomons, W.; Forstner, U. *Metals in the Hydrocycle*; Springer Science & Business Media: Berlin/Heidelberg, Germany, 2012.
39. Adriano, D.C. *Trace Elements in the Terrestrial Environment*; Springer Science & Business Media: Berlin/Heidelberg, Germany, 2013.
40. Chen, H.; Teng, Y.; Lu, S.; Wang, Y.; Wang, J. Contamination features and health risk of soil heavy metals in China. *Sci. Total Environ.* **2015**, *512–513*, 143–153. [[CrossRef](#)] [[PubMed](#)]
41. Xi, X.H.; Hou, Q.Y.; Yang, Z.F.; Ye, J.Y.; Yu, T.; Xia, X.Q.; Cheng, H.X.; Zhou, G.H.; Yao, L. Big data based studies of the variation features of Chinese soil's background value versus reference value: A paper written on the occasion of Soil Geochemical Parameters of China's publication. *Ceophys. Geochem. Explor.* **2021**, *45*, 1095–1108.
42. Georges, S.; Vera, M.; Florias, M. *Interpretation of Micromorphological Features of Soils and Regoliths*, 2nd ed.; Elsevier: Amsterdam, The Netherlands, 2018.
43. Li, M.; Xi, X.H.; Xiao, G.; Cheng, H.X.; Yang, Z.F.; Zhou, G.; Ye, J.Y.; Li, Z. National multipurpose regional geochemical survey in China. *J. Geochem. Explor.* **2014**, *139*, 21–30. [[CrossRef](#)]
44. Ji, H.B.; Wang, S.J.; Ouyang, Z.Y. Geochemistry of red residua underlying dolomites in karst terrains of Yunnan–Guizhou Plateau: I. The formation of the Pingba profile. *Chem. Geol.* **2004**, *203*, 1–27. [[CrossRef](#)]
45. Ji, H.B.; Wang, S.J.; Ouyang, Z.Y. Geochemistry of red residua underlying dolomites in karst terrains of Yunnan–Guizhou Plateau II. The mobility of rare earth elements during weathering. *Chem. Geol.* **2004**, *203*, 29–50. [[CrossRef](#)]
46. Ji, W.B.; Ying, R.R.; Yang, Z.F.; Yang, Q.; Liu, X.; Yu, T.; Wang, L.; Qin, J.X.; Wu, T.S. Arsenic Concentration, Fraction, and Environmental Implication in Fe–Mn Nodules in the Karst Area of Guangxi. *Water* **2022**, *14*, 3021. [[CrossRef](#)]
47. Ji, W.B.; Lu, Y.Y.; Zhao, C.Y.; Zhang, X.Y.; Wang, H.; Hu, Z.W.; Yu, T.; Wen, Y.B.; Ying, R.R.; Yang, Z.F. Mineral Composition and Environmental Importance of Fe–Mn Nodules in Soils in Karst Areas of Guangxi, China. *Sustainability* **2022**, *14*, 12457. [[CrossRef](#)]
48. Suda, A.; Makino, T. Functional effects of manganese and iron oxides on the dynamics of trace elements in soils with a special focus on arsenic and cadmium: A review. *Geoderma* **2016**, *270*, 68–75. [[CrossRef](#)]
49. Ettler, V.; Tomášová, Z.; Komárek, M.; Mihaljevič, M.; Šebek, O.; Michálková, Z. The pH-dependent long-term stability of an amorphous manganese oxide in smelter-polluted soils: Implication for chemical stabilization of metals and metalloids. *J. Hazard. Mater.* **2015**, *286*, 386–394. [[CrossRef](#)]
50. Ettler, V.; Chren, M.; Mihaljevič, M.; Drahotka, P.; Kříbek, B.; Veselovský, F.; Sracek, O.; Vaněk, A.; Penížek, V.; Komárek, M.; et al. Characterization of Fe–Mn concentric nodules from Luvisol irrigated by mine water in a semi-arid agricultural area. *Geoderma* **2017**, *299*, 32–42. [[CrossRef](#)]

51. Li, C.; Zhang, C.S.; Yu, T.; Ma, X.D.; Yang, Y.Y.; Liu, X.; Hou, Q.Y.; Li, B.; Lin, K.; Yang, Z.F.; et al. Identification of soil parent materials in naturally high background areas based on machine learning. *Sci. Total Environ.* **2023**, *875*, 162684. [[CrossRef](#)] [[PubMed](#)]
52. Sipos, P.; Kovács, I.; Balázs, R.; Tóth, A.; Barna, G.; Makó, A. Micro-analytical study of the distribution of iron phases in ferromanganese nodules. *Geoderma* **2022**, *405*, 115445. [[CrossRef](#)]

**Disclaimer/Publisher's Note:** The statements, opinions and data contained in all publications are solely those of the individual author(s) and contributor(s) and not of MDPI and/or the editor(s). MDPI and/or the editor(s) disclaim responsibility for any injury to people or property resulting from any ideas, methods, instructions or products referred to in the content.